

Original Article

High mobility group box1 protein is involved in acute inflammation induced by *Clostridium difficile* toxin A

Ji Liu¹, Bei-Lei Zhang¹, Chun-Li Sun¹, Jun Wang², Shan Li^{1,3,*}, and Ju-Fang Wang^{1,*}

¹School of Bioscience & Bioengineering, South China University of Technology, Guangzhou 510006, China,

²Shenzhen Huada Gene Research Institute, Shenzhen 518083, China, and ³Guangdong Province Key Laboratory of Fermentation and Enzyme Engineering, South China University of Technology, Guangzhou 510006, China

*Correspondence address. Tel/Fax: +86-20-39380626; E-mail: lishan@scut.edu.cn (S.L.)/jufwang@scut.edu.cn (J.W.)

Received 25 November 2015; Accepted 31 March 2016

Abstract

High mobility group box1 (HMGB1), as a damage-associated inflammatory factor, contributes to the pathogenesis of numerous chronic inflammatory and autoimmune diseases. In this study, we explored the role of HMGB1 in CDI (*Clostridium difficile* infection) by *in vivo* and *in vitro* experiments. Our results showed that HMGB1 might play an important role in the acute inflammatory responses to *C. difficile* toxin A (TcdA), affect early inflammatory factors, and induce inflammation via the HMGB1-TLR4 pathway. Our study provides the essential information for better understanding the molecular mechanisms of CDI and the potential new therapeutic strategies for the treatment of this infection.

Key words: inflammation, *Clostridium difficile* toxin A, HMGB1, ileal loop

Introduction

The anaerobic Gram-positive bacterial species *Clostridium difficile* is the most common cause of nosocomial antibiotic-associated diarrhea and pseudomembranous colitis [1]. The recent emergence of hypervirulent strains has caused a rapid increase in the incidence of *C. difficile* infection (CDI) worldwide, along with the development of more severe forms of the disease [2–4].

CDI is primarily caused by two large proteins, *C. difficile* toxin A (TcdA) and *C. difficile* toxin B (TcdB) with molecular weights of 308 and 270 kDa, respectively. TcdA is traditionally recognized as an enterotoxin and believed to play a more important role in the pathogenesis of CDI than TcdB. It causes fluid accumulation and disrupts the cytoskeleton of intestinal epithelial cells, triggering intestinal injury and the release of proinflammatory cytokines such as interleukin (IL)-1 β , IL-6, and tumor necrosis factor- α (TNF- α) [5].

High mobility group box1 (HMGB1) is a highly conserved protein that is ubiquitously expressed in the nucleus and cytoplasm of

cells [6]. It functions as a mediator in both acute and chronic inflammatory responses, such as sepsis and arthritis [7,8], and plays a role in the pathogenesis of atherosclerosis and cancer [9,10]. Recent studies have suggested that HMGB1 acts as an early mediator in regulating inflammation and tissue damage in hepatic ischemia-reperfusion injury [11,12]. After being released from the cell, extracellular HMGB1 interacts with toll-like receptor 4 (TLR4), a mediator of innate immune responses, leading to the activation of signaling cascades and the production of proinflammatory cytokines [13].

Glycyrrhizin, a natural anti-inflammatory and antiviral triterpene, inhibits HMGB1 activity by binding directly to HMGB1 and interacting with the two HMG boxes without distorting their secondary structure, which allows it to attenuate HMGB1-induced inflammation. Therefore, it is regarded as a candidate inhibitor of the HMGB1-dependent inflammatory axis [14,15]. CLI-095, a small molecule, which selectively inhibits TLR4 signaling by binding to

the TLR4 receptor complex, could be a promising therapeutic agent for the treatment of inflammatory diseases in which the pathogenesis involves TLR4 [16–18].

In this study, we explored the role of HMGB1 in TcdA-induced inflammation. The results showed that HMGB1 is an inflammation factor, which can induce acute inflammation and intestinal injury. HMGB1 is involved in the acute inflammation induced by TcdA via HMGB1-TLR4 pathway. Inhibition of HMGB1-TLR4 pathway alleviates TcdA-induced inflammation and intestinal injury, suggesting that HMGB1 may be a potential therapeutic target for the treatment of CDI.

Materials and Methods

Cell culture and TcdA purification

The murine colon adenocarcinoma cell line CT26, human colon adenocarcinoma cell line HCT8, and mouse monocyte macrophage leukemia cell line RAW264.7 were obtained from American Type Culture Collection (Manassas, USA) and cultured in Dulbecco's Modified Eagle's medium (GIBCO, Carlsbad, USA) containing 10% fetal bovine serum (GIBCO), 100 U/ml penicillin, 100 µg/ml streptomycin, 2 mM L-glutamine and 1 mM sodium pyruvate (GIBCO). The full-length wild-type recombinant TcdA plasmid was kindly provided by Dr. Feng (University of Maryland at Baltimore, Baltimore, USA). TcdA was expressed and purified according to the protocol reported by Sullivan *et al.* [19]. The highly purified recombinant TcdA appeared as a single band on sodium dodecyl sulfate polyacrylamide gels (data not shown). rHMGB1 was purchased from Uscn Life Science Inc (Wuhan, China).

Animals

CD1 mice (5- to 6-week-old, female) were purchased from Medical Experimental Animal Center (Guangzhou, China) and housed in a dedicated pathogen-free facility according to China Animal Care and Use Committee guidelines. All animals were handled according to the Institutional Animal Care guidelines.

Cell rounding assay

CT26 cells were seeded in 96-well plates (1×10^4 cells/well), and then exposed to TcdA (10 ng/ml) for 4 h or pretreated with 100 µM glycyrrhizin (30 min) before TcdA exposure. Cell rounding was visualized by phase-contrast microscopy. Each concentration was tested in triplicate for overall cell rounding, and the experiments were repeated three times.

Western blot analysis

CT26 cells were treated with TcdA at the concentration of 10 ng/ml, the culture medium was collected at 0, 4, 8, 12, 16, and 24 h. Proteins were separated on 12% sodium dodecyl sulphate-polyacrylamide gel electrophoresis (SDS-PAGE) and electrophoretically transferred to nitrocellulose filter membranes. The membranes were blocked with 5% bovine serum albumin. And then the membranes were incubated overnight at 4°C with the indicated primary antibodies (anti-HMGB1 antibody, 1:1000; Cell Signaling, Beverly, USA), anti-BSA antibody (1:1000; Santa Cruz, Santa Cruz, USA). After being washed three times, the membranes were treated with horseradish peroxidase-conjugated secondary antibodies (1:2000; Cell Signaling) and the bands were visualized using the enhanced chemiluminescence kit (Thermo, Rockford, USA).

Mouse ileal loop model

CD1 mice were maintained in a conventional housing unit and fasted for 8 h before surgery. The HMGB1 inhibitor glycyrrhizin (50 mg/kg; Sigma-Aldrich, St Louis, USA), or TLR4 inhibitor CLI-095 (40 µg/kg; Sigma-Aldrich), was injected intraperitoneally once daily for 2 days before ileal loop surgery. Pentobarbital anesthesia (90 mg/kg) was injected intraperitoneally. After a midline laparotomy, two distal 2- to 3-cm ileal loops were ligated and injected with 10 µg of wild-type TcdA dissolved in 100 µl phosphate buffered saline (PBS). Control loops were injected with PBS only. After 4 h, the mice were euthanized, and the ileal loops were removed for subsequent analysis. The loop lengths and weights were measured, and fluid secretion was assessed based on the ratio of loop weight (mg) to loop length (cm).

Tissue myeloperoxidase assay

Tissue myeloperoxidase (MPO) activity was determined as described previously [20]. To measure MPO (neutrophil myeloperoxidase) activity, part of the resected ileum was freeze-dried and homogenized in 1 ml of PBS containing 0.5% hexadecyltrimethylammonium bromide and 5 mM EDTA. The tissues were disrupted by sonication and freeze-thaw cycles. MPO activity in the supernatant was determined using *o*-phenylenediamine in a solution containing 0.05% H₂O₂ as substrate, followed by measurement of the absorbance of the samples at 490 nm using a plate reader (Synergy HT; Bio-Tek, Winooski, USA). MPO activity was expressed as milligram per gram of tissue.

Hematoxylin and eosin analysis

Histopathological assay was performed to evaluate mucosal damage induced by the toxins. Resected ileal loops were fixed in 4% formaldehyde buffered with PBS and then embedded with paraffin. Deparaffinized 6-µm-thick sections were stained with hematoxylin and eosin (H&E) for histological analysis. Briefly, slides were scored by two independent investigators who were blinded to the study groups. Histological damage was scored on a 0–3 scale as follows: absence of inflammation and damage was scored 0, and mild, moderate, and severe inflammatory were scored 1, 2, and 3, respectively.

Real-time polymerase chain reaction analysis

Total RNA was extracted from the intestine tissue using an RNeasy Plus Mini kit (TaKaRa, Dalian, China). The RNA was further treated with RQ1 RNase-free DNase (TaKaRa) to remove DNA contamination. The purified RNA (1 µg) was reverse transcribed to obtain cDNA using M-MLV reverse transcriptase (Invitrogen, Carlsbad, USA) with oligo (dT) for 1 h at 37°C. Then a mastermix (TaKaRa) of the following components was prepared to the indicated final concentration: 2.5 mM MgCl₂, 0.2 µM forward primers, 0.2 µM reverse primer, plus 2.0 µl SYBR Green I (TaKaRa). The mastermix was filled in the capillaries (Bio-Rad, Hercules, USA) and 1 µl cDNA was added as the template. Real-time polymerase chain reaction (PCR) amplification was performed using the following conditions for 40 cycles: 95°C for 5 s, 60°C for 30 s, on the LightCycler (Roche Diagnostics, Indianapolis, USA). For the mathematical model, it is necessary to determine the crossing points for each transcript. And the primers used in PCR reaction were listed in Table 1.

Immunoprecipitation

The immunoprecipitation was carried out as described previously [21]. RAW264.7 cells were incubated for the indicated time with the lysates of TcdA-treated intestinal tissues, which had been pretreated with glycyrrhizin or PBS, and then were lysed in lysis buffer containing a protease inhibitor cocktail. Whole-cell extracts were centrifuged at 14,000 g for 20 min to remove debris. A total of 15 μ l protein A/G plus-agarose beads was added to the mixture followed by incubation with anti-HMGB1 antibody at 4°C on a rocker platform overnight. Beads were pelleted by centrifugation at 1000 g for 5 min at 4°C, and the pellets were washed three times with 1.0-ml ice-cold RIPA buffer. Supernatants were discarded and pellets were resuspended in 20 μ l of 2 \times electrophoresis sample buffer. The samples were boiled for 5 min at 95°C to dissociate the immunocomplex from the beads. Then, samples were centrifuged at 10,000 g for 2 min to pellet the agarose beads and the supernatant was subject to 12% SDS-PAGE, followed by western blot analysis with anti-HMGB1 antibody (1:1000; Cell Signaling Technology) and anti-TLR4 antibody (1:1000; Abcam, Cambridge, UK).

Intestinal barrier function analysis

HCT8 cells (1×10^4 cells/well) were plated on permeable filters in 12-well Transwell bicameral chambers (Corning Co, Corning, USA). Permeability studies were performed using confluent monolayers between 4 and 7 days after seeding. The permeability probe was fluorescein isothiocyanate-labeled dextran (4000 Da, FD4). FD4 (0.2 mg/ml) was added into the transwells. After 24 h, the media was collected to measure the fluorescence value of the samples.

Table 1. The primer sequences for amplifying the mRNA of inflammatory factors

Inflammatory factors	Primer
<i>IL-1β</i>	Sense: 5'-CCCCAACTGGTACATCA-3' Anti-sense: 5'-AGGTAAGTGGTTGCCC-3'
<i>IL-6</i>	Sense: 5'-ATGATGGATGCTACCAAAC-3' Anti-sense: 5'-AGGCATAACGCACTAGG-3'
<i>TNF-α</i>	Sense: 5'-CAGCCTCTTCTCATTCTGCTTGTG-3' Anti-sense: 5'-CTGGAAGACTCTCCAGGTATAT-3'
<i>KC</i>	Sense: 5'-GAGCCTCTAACCAGTTCC-3' Anti-sense: 5'-TCCACGACATACTCAGCAC-3'

Statistical analysis

Unless indicated, experiments were repeated at least three times. Data were expressed as the mean \pm SEM. Data were analyzed using Prism v.5.03 (GraphPad Software, San Diego, USA). Statistical significance was assessed by one-way analysis of variance (ANOVA) followed by Turkey's test, or two-way repeated-measures ANOVA. $P < 0.05$ was considered as statistically significant.

Results

TcdA exposure induces HMGB1 release from CT26 cells

The effect of TcdA on CT26 cells was examined by cell rounding assay. The results showed that TcdA-induced cell rounding in a dose-dependent manner, with 60% cell rounding observed after being exposed to 1 ng/ml of TcdA and 100% cell rounding to 10 ng/ml of TcdA for 4 h (Fig. 1A). To measure HMGB1 secretion in TcdA-treated cells, CT26 cells were cultured in the presence of 10 ng/ml of TcdA and the medium was collected at the indicated time. Western blot analysis showed that HMGB1 was released from the nucleus to cytoplasm when cells were exposed to TcdA for 4 h (Fig. 1B). And the content of HMGB1 in medium was increased in a time-dependent manner after 8 h of exposure (Fig. 1C).

Exogenous rHMGB1 induces inflammation and intestinal injury

To determine the effect of HMGB1 on acute inflammation, rHMGB1 (10^{-12} pg/100 μ l) was used to verify tissue damage and inflammation in the 'ileal loop' surgical model. As shown in Fig. 2A, the ligated ileal loops showed fluid accumulation and intestinal injury after rHMGB1 exposure for 4 h. The W/L ratio for the rHMGB1 group was approximately 170. The W/L ratio in the PBS group was only 30.

Ileal loop tissues in rHMGB1 treatment group showed increased MPO activity (Fig. 2B). The MPO value was approximately 200 ng/g. By contrast, MPO value for the PBS group was as low as 40 ng/g.

Histopathological examination revealed that rHMGB1 may cause severe damage to the architecture of intestinal villi (Fig. 2C). The histopathological score of rHMGB1 group was 2.4. By contrast, a normal lumen structure was observed for loops in PBS group and the score was about 0.1.

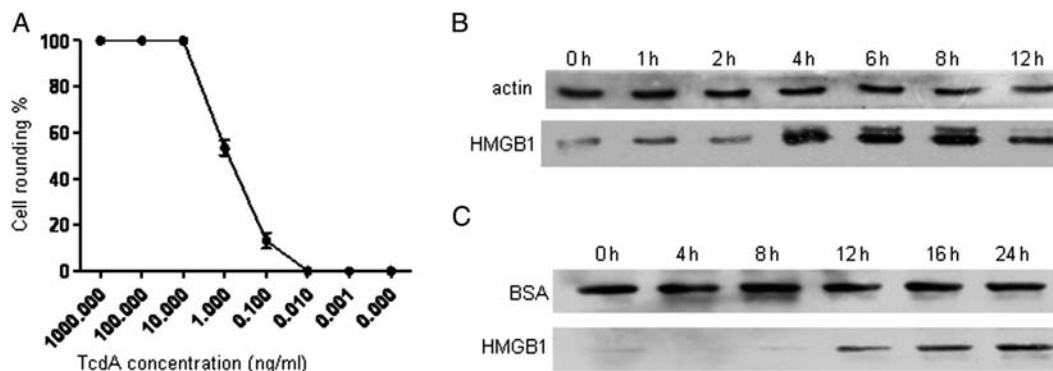


Figure 1. TcdA induces the release of HMGB1 from CT26 cells (A) CT26 cells were treated with different concentrations of TcdA for 4 h, and the rate of cell rounding was calculated. (B) After CT26 cells were exposed to 10 ng/ml of TcdA for the indicated times, the cell lysates were collected. The HMGB1 levels in the cytoplasm were detected by western blot analysis. (C) CT26 cells were exposed to 10 ng/ml of TcdA for the indicated time intervals, and HMGB1 levels in the culture medium were detected by western blot analysis using BSA as a loading control.

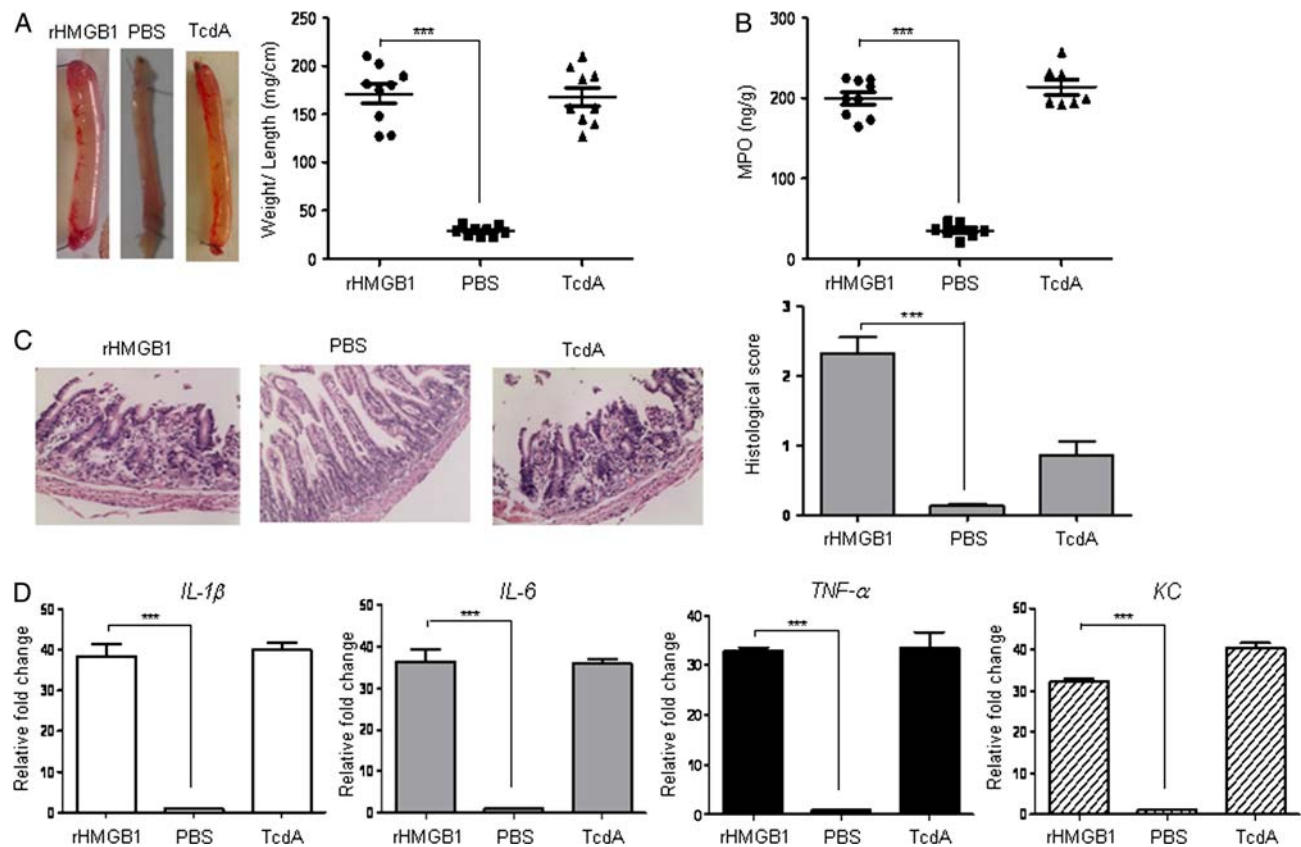


Figure 2. Effects of HMGB1 on mouse ligated ileal loops rHMGB1, PBS, or TcdA was injected into the ligated ileal loops, then mice were sacrificed and the ileal loops were collected for subsequent analysis. (A) Intestinal fluid accumulation was quantified by the loop weight (mg) to length (cm) ratio. Representative loops are shown. (B) Intestinal tissue from loops injected with rHMGB1 or TcdA was homogenized, and MPO activity was calculated from a standard curve generated using the purified MPO. (C) H&E staining and mean histology scores (range 0–3) of sections of TcdA- or HMGB1-treated ilea. (D) mRNA expressions of *IL-1 β* , *IL-6*, *TNF- α* , and *KC* were evaluated in the ileal segments by real-time PCR. GAPDH was used as the loading control. Data represent the mean of three independent experiments. *** $P < 0.001$.

The mRNA expressions of proinflammatory cytokine genes (*TNF- α* , *IL-1 β* , *IL-6*, *KC*) were evaluated in the ileal segments by real-time PCR. As shown in Fig. 2D, the expression levels of cytokines in the TcdA exposure group were significantly increased. And the cytokine expressions in the rHMGB1 group were not significantly different from those in the TcdA group.

Glycyrrhizin alleviates HMGB1-induced acute inflammation and intestinal injury

As shown in Fig. 3A, the ligated ileal loops showed fluid accumulation after exposure to 10^{-12} pg/100 μ l of rHMGB1 for 4–6 h. However the mixture of glycyrrhizin (100 mM) and rHMGB1 (10^{-12} pg/100 μ l) could reduce fluid accumulation. The W/L ratio of rHMGB1 group was approximately 170, whereas the W/L ratio of mixture group decreased to 40, which was similar to that of PBS group. An increased MPO value (about 220 ng/g) was observed in rHMGB1 group (Fig. 3B). Neutrophil influx was confirmed by a substantial decrease in MPO activity in the mixture group, with an 80% decrease down to 40 ng/g. By contrast, MPO value for both the glycyrrhizin group and PBS only group was approximately 40 ng/g.

Histopathological examination revealed that exposure to rHMGB1 may cause severe damage to epithelia (Fig. 3C). Histopathological score of rHMGB1 group was 2.4. By contrast, a normal lumen structure was observed for loops treated with the

mixture of rHMGB1 and glycyrrhizin, similar to that of the PBS group with a score of about 0.1.

Quantitative mRNA analysis of proinflammatory cytokines (*TNF- α* , *IL-1 β* , *IL-6*, and *KC*) revealed that rHMGB1 stimulated the expression of cytokines in ileal segments, in contrast to that of the PBS group. No significant difference was observed between the glycyrrhizin group and the HMGB1 + glycyrrhizin mixture group (Fig. 3D). The expressions of cytokines in the HMGB1 + glycyrrhizin mixture group were decreased to normal level, which is similar to those in PBS group.

Glycyrrhizin pretreatment affects TcdA-induced intestinal inflammation and tissue damage in the murine ileum

HMGB1 is released from cells exposed to TcdA and further induces acute inflammation in intestinal tissue (Fig. 3). So we pretreated the cells separated from intestinal tissues with glycyrrhizin prior to TcdA exposure to inhibit the activity of the subsequently secreted HMGB1, and further observed the relationship between HMGB1 and TcdA-induced inflammation. As shown in Fig. 4A, the ligated ileal loops induced serious swelling and increased fluid accumulation after 4 h of treatment with 10 μ g TcdA, compared with glycyrrhizin pretreatment group. The W/L value of glycyrrhizin pretreatment group was significantly decreased by more than 80% to about 30,

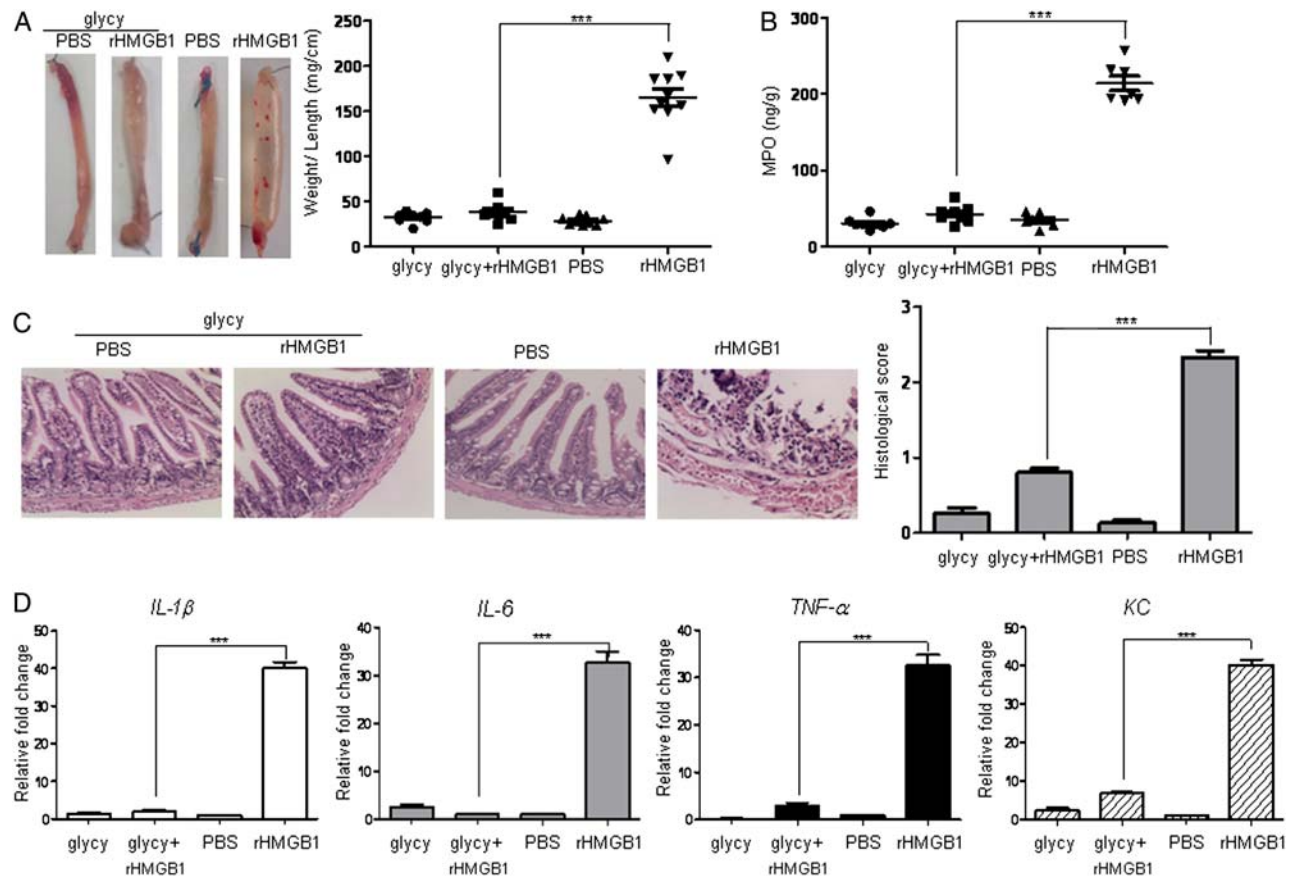


Figure 3. Glycyrrhizin alleviates HMGB1-induced enterotoxicity rHMGB1, glycyrrhizin, or rHMGB1 combined with glycyrrhizin was injected into the ligated ileal loops, then mice were sacrificed and the ileal loops were collected for subsequent analysis. (A) Intestinal fluid accumulation was quantified by the loop weight (mg) to length (cm) ratio. Representative loops are shown. (B) Intestinal tissue from loops injected with HMGB1 or glycyrrhizin was homogenized and MPO activity was calculated from a standard curve generated using the purified MPO. (C) H&E staining and mean histology scores (range 0–3) of sections of glycyrrhizin- or HMGB1-treated ilea. (D) mRNA expressions of *IL-1 β* , *IL-6*, *TNF- α* , and *KC* in ileal tissues treated as indicated were measured by real-time PCR. *GAPDH* was used as the loading control. Data represent the mean of three independent experiments. *** $P < 0.001$.

compared with that of the TcdA control, which is 175. By contrast, without TcdA exposure, the glycyrrhizin or PBS group's W/L value was approximately 30.

The MPO activity of TcdA group was significantly increased to about 230 ng/g, indicating that TcdA may induce the influx of neutrophils (Fig. 4B). However, in the glycyrrhizin pretreatment group, the MPO value was decreased to 60 ng/g, whereas the value in the glycyrrhizin group or PBS only group was approximately 20 ng/g (Fig. 4B).

Moreover, the glycyrrhizin pretreatment group showed a normal lumen structure of loops. Histopathological score of TcdA group and glycyrrhizin pretreatment group was about 2.3 and 0.8, respectively (Fig. 4C).

Finally, the mRNA level of proinflammatory cytokines including *TNF- α* , *IL-1 β* , *IL-6*, and *KC* were evaluated in the ileal segments by real-time PCR. As shown in Fig. 4D, the expression levels of cytokines in the TcdA exposure group were significantly increased. And cytokine expressions in the glycyrrhizin pretreatment group were decreased to normal levels.

Glycyrrhizin inhibits the activity of HMGB1 in intestinal tissues *in vivo* and *in vitro*

In order to investigate the involvement of HMGB1 in TcdA-induced tissue damage, both *in vitro* and *in vivo* experiments were designed.

First, HCT8 colonic monolayer was used to verify the results *in vitro*. As shown in Fig. 5A, confluent HCT8 monolayers were incubated for 24 h with TcdA or rHMGB1. rHMGB1 increased the permeability of HCT8 monolayer, which was demonstrated by FD4 increase. A similar pattern was observed when monolayers were incubated with TcdA. But after pretreatment with glycyrrhizin, the permeability of monolayers remained unchanged. And the same result was observed in the HMGB1 + glycyrrhizin mixture group.

Next, the ileal loops were used to explore HMGB1 in TcdA-induced tissue damage *in vivo*. The concentration of HMGB1 in the whole intestinal tissue (ileum loop tissue) remained constant in TcdA, PBS, TcdA + glycyrrhizin, and PBS+glycyrrhizin groups (Fig. 5B). It was found that treatment with glycyrrhizin could not reduce concentration of HMGB1 in tissue. But in tissue cells, the secretion of HMGB1 from nuclear into cytoplasm in the TcdA treatment group was increased compared with that in the PBS group (Fig. 5C).

Then, immunoprecipitation was used to detect the activity of HMGB1 in intestinal tissue. The amount of HMGB1 and TLR4 complex indicated HMGB1 activity. As shown in Fig. 5D, western blot assay revealed that amount of HMGB1 and TLR4 complex in glycyrrhizin pretreatment group was significantly lower than that in PBS group. It is supposed that glycyrrhizin may bind to the secreted HMGB1, which competitively inhibits the binding of HMGB1 to TLR4.

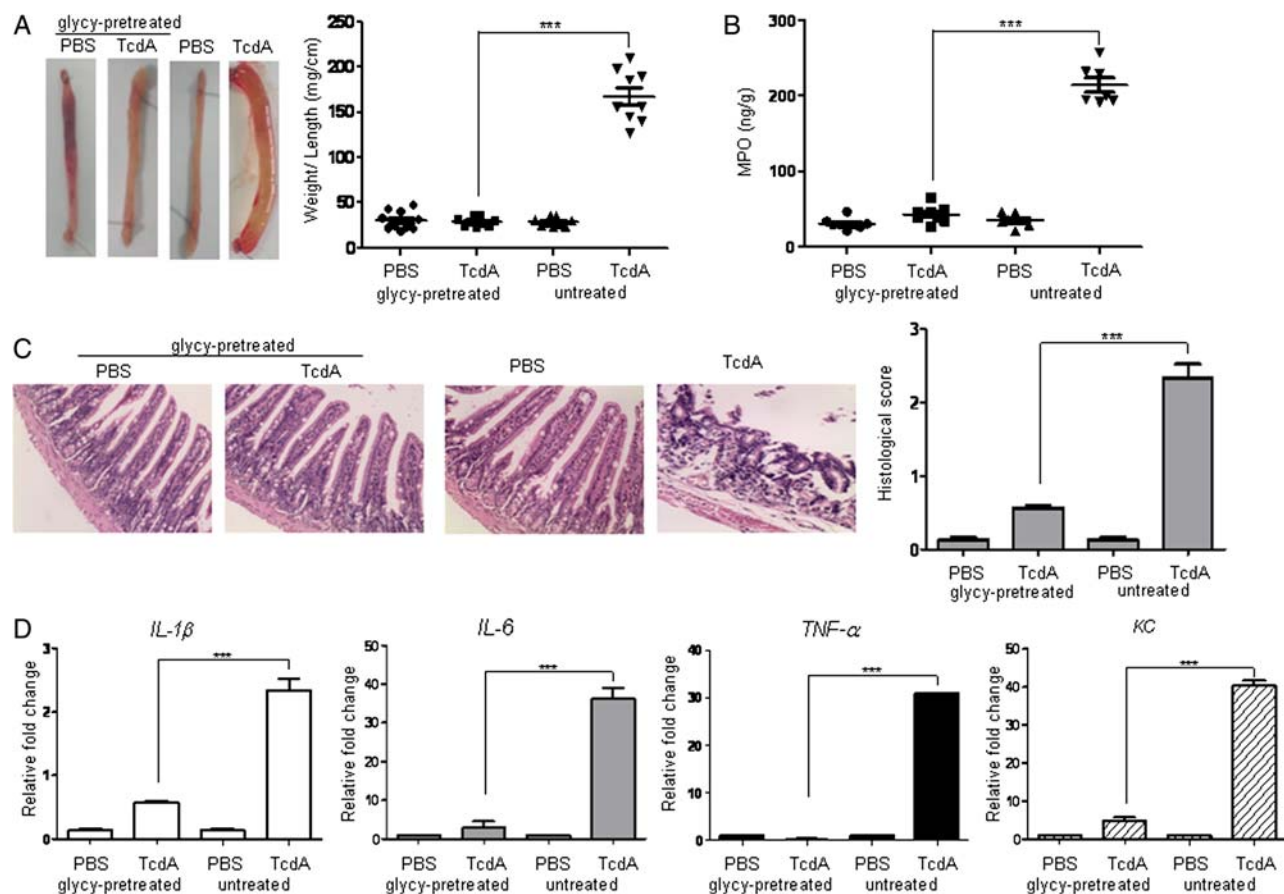


Figure 4. Effect of glycyrrhizin pre-treatment on TcdA-induced enterotoxicity Mice were pretreated with glycyrrhizin for 2 days before the operation. Wild-type TcdA or vehicle control (PBS) was injected into ligated ileal loops, then mice were sacrificed and the ileal loops were collected for subsequent analysis. (A) Intestinal fluid accumulation was quantified by the loop weight (mg) to length (cm) ratio. Representative loops injected with PBS or TcdA are shown. (B) Intestinal tissue from loops injected with PBS or TcdA was homogenized and MPO activity was calculated from a standard curve generated using the purified MPO. (C) H&E staining of the sections and mean histology scores (range 0–3) of sections from PBS- or toxin-treated ilea. (D) mRNA expressions of *IL-1 β* , *IL-6*, *TNF- α* , and *KC* in ileal tissues after PBS or toxin treatment were measured by real-time PCR. *GAPDH* was used as the loading control. Data represent the mean of three independent experiments. *** $P < 0.0001$.

Effect of TLR4 inhibitor on HMGB1-induced enterotoxicity

Further experiments were carried out to investigate if TLR4 inhibitor CLI-095 could alleviate HMGB1-induced acute inflammation and intestinal injury. As shown in Fig. 6A, significant differences were found between the TLR4 inhibitor pretreatment group and the control group. The W/L value in the CLI-095 pretreated group was 30, <80% of that in TcdA group. Figure 6B showed that the influx of neutrophils was decreased significantly in CLI-095 group compared with that in the TcdA group with an MPO value of approximately 40 ng/g, while the MPO value in TcdA group was approximately 200 ng/g (Fig. 6B). The Histological score of TcdA group was 2.2, while the score of the CLI-095 pretreated group was 0.6 (Fig. 6C). The exogenous rHMGB1 was also used in the same experiments, CLI-095 treatment before exogenous rHMGB1 exposure also alleviated HMGB1-induced inflammation (data not show).

Discussion

The incidence of CDI-associated mortality has increased rapidly in recent years [19]; however, the molecular mechanisms underlying the pathogenesis of CDI remain unclear. In this study, we found that

HMGB1, an inflammatory factor, played an important role in the acute inflammatory response to TcdA, affecting early-acting proinflammatory cytokines via the HMGB1-TLR4 pathway. These results could provide essential information for better understanding the molecular mechanisms of CDI and explore the potential new therapeutic strategies for the treatment of this infection.

Early studies have shown that HMGB1 is released from intestinal and involved in toxin-induced inflammation [20,22]. In this study, we found that HMGB1 was released from the nucleus to the cytoplasm after 4 h of TcdA exposure, then from cytoplasm to culture medium after 8 h of TcdA exposure. Glycyrrhizin can attenuate the activity of HMGB1. Our results showed that glycyrrhizin pretreatment delayed the onset of TcdA-induced cell rounding (data not shown). These results imply that HMGB1 is probably involved in the cytotoxic and cytopathic effects of TcdA.

The 'ileal loop' surgical model is a well-established model for analyzing acute tissue damage and inflammatory responses to TcdA and evaluating therapeutic approaches *in vivo*, as well as for the characterization of enterotoxins [5,16]. In this study, this model was adopted and the results showed that HMGB1 plays a critical role in the activation of inflammation. In addition to up-regulating MPO and cytokine expression, and damaging the architecture of intestinal villi (Fig. 2), rHMGB1 also significantly induced neutrophil

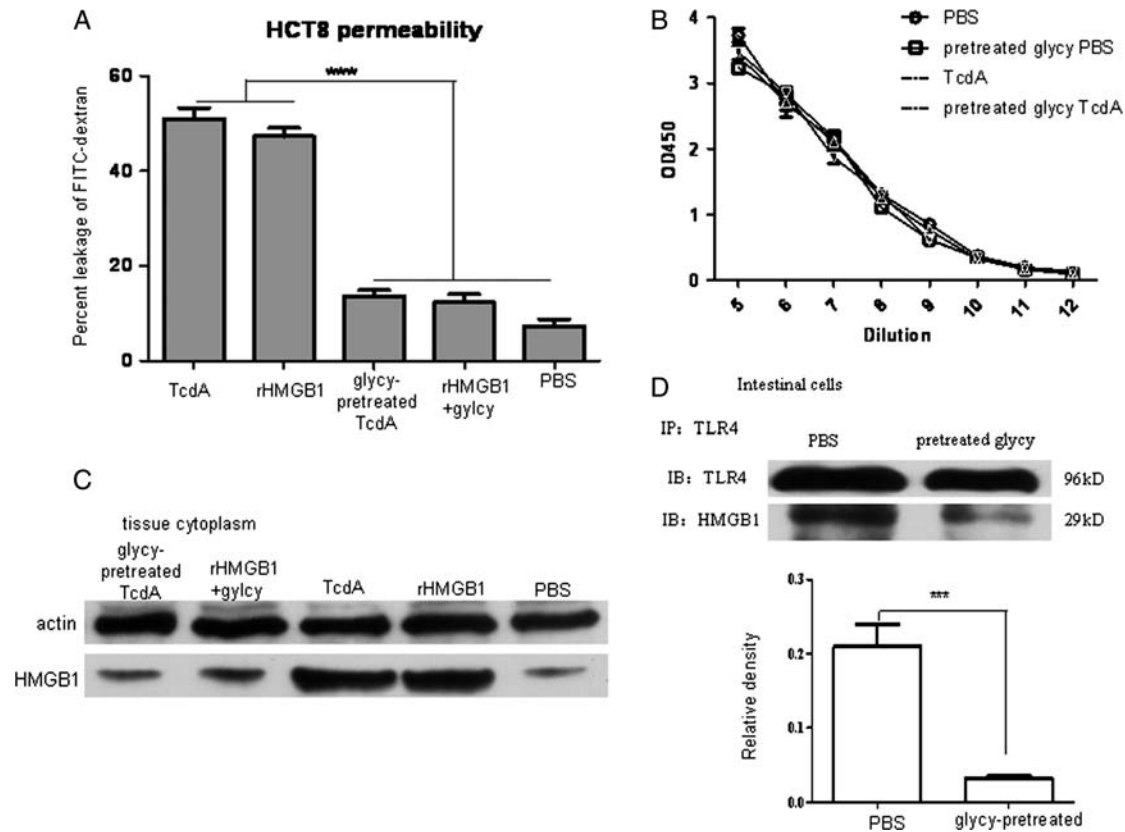


Figure 5. HMGB1 concentration and activity in intestinal tissues (A) Effect of HMGB1 or TcdA on HCT8 permeability. (B) Mice were pretreated with glycyrrhizin for 2 days before the operation. The ileal loop tissues were removed from mice after toxin A or PBS treatment for 4 h. Tissues were lysed and diluted to different concentrations before measurement of HMGB1 by ELISA. (C) HMGB1 levels in the cytoplasm were detected by western blot analysis. (D) RAW264.7 cells were incubated with intestinal cell lysates, and HMGB1 was detected by western blot analysis after immunoprecipitation using an antibody against TLR4. Representative blots and densitometric analysis are shown. Data represent of a typical experiment out of three independent experiments. *** $P < 0.001$.

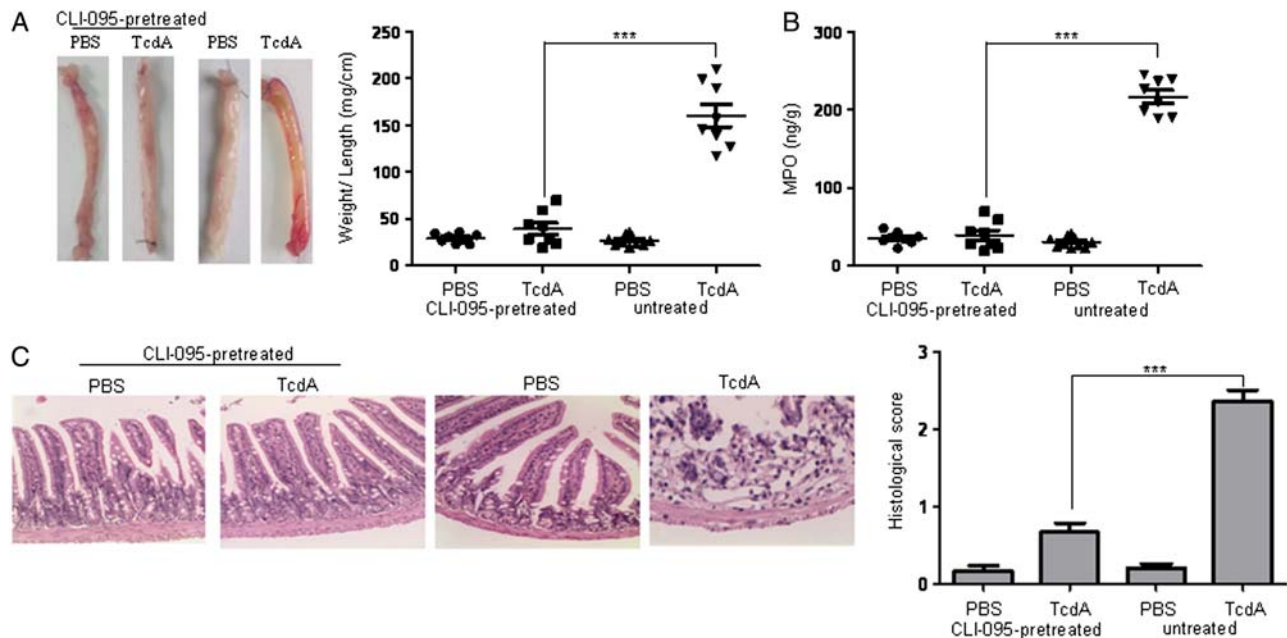


Figure 6. Effect of TLR4 inhibition on HMGB1-induced enterotoxicity Mice were pretreated with the TLR4 inhibitor CLI-095 for 2 days before the operation. rHMGB1 or PBS was injected into ligated ileal loops, the mice were sacrificed, and the ileal loops were collected for subsequent analysis. (A) Intestinal fluid accumulation was quantified by the loop weight (mg) to length (cm) ratio. Representative loops are shown. (B) Intestinal tissue from loops injected with HMGB1 or PBS was homogenized and MPO activity was calculated from a standard curve generated using the purified MPO. (C) H&E staining and mean histology scores (range 0–3) of sections of PBS- or CLI-095-treated ilea. *** $P < 0.001$.

accumulation and aggravated the severity of edema, which is similar to the effect of the toxin A.

HMGB1 has key functions within the nucleus: it stabilizes the nucleosome structure and facilitates intracellular gene transcription [22,23]. HMGB1 release massively into the extra-cellular environment when cell dying, and extra-cellular HMGB1 acts as a chemotactant and takes cytokine like function for inflammatory [23]. HMGB1 is a cytokine capable of inducing alterations in intestinal barrier function both *in vitro* and *in vivo* [24]. Our results suggested that HMGB1 has an impact on intestinal epithelial barrier function (Fig. 5A). Inhibition of HMGB1 could lead to reduction of the expressions of proinflammatory cytokines (Fig. 3D), suggesting that HMGB1 may be an important inflammation factor involved in CDI.

The interaction between HMGB1 and TLR4 leads to increased production and secretion of cytokines in macrophages and neutrophils [25,26]. Our results indicated that glycyrrhizin could prevent HMGB1 from binding to TLR4 (Fig. 5D), and down-regulate the expressions of the cytokines (data not shown), suggesting that the binding of HMGB1 to TLR4 may be closely related to inflammation and tissue damage, and TLR4 is required to initiate an appropriate innate immune response to *C. difficile* in an infection model. Figure 6 further showed that HMGB1 may function as a mediator in TcdA-induced response through the HMGB1-TLR4 pathway. TLR4 inhibitor CLI-095 was found to alleviate HMGB1-induced acute inflammation and intestinal injury.

Ryan *et al.* [27] showed that the TLR4^{-/-} mice were more susceptible to an active CDI, suggesting that the toxin exposure models may not reflect the pathophysiology of an active CDI. The role played by TLR4 in pathophysiology in human models needs to be further explored in future.

TcdA was found to induce caspase-3/7 activation when the toxin was applied at the concentration of 100 nM [22]. We also demonstrated that TcdA-induced tumor death was an apoptosis process, while pretreatment with caspase inhibitor Z-VAD-fmk effectively inhibited CT26 tumor death (Supplementary Fig. S1).

In summary, this study provides further evidence that HMGB1 plays a part in acute inflammatory response to TcdA, and plays an important role in acute inflammatory. Our findings provide insight into the molecular mechanisms underlying the pathogenesis of CDI and useful information for the design of novel therapeutic strategies for the treatment of TcdA-induced acute inflammation and intestinal injury.

Supplementary Data

Supplementary data is available at *ABBS* online.

Acknowledgments

We would like to thank Dr. Hanping Feng from Department of Microbial Pathogenesis, University of Maryland Dental School (Baltimore, USA) for the technical assistance.

Funding

This work was supported by the grants from the International Cooperation Programme of Department of Science and Technology of Guangdong Province (No. 2015E8151400), Innovative Program of Department of Education of Guangdong Province (No. 2013KJCX0013), and Fermentation and Enzyme Engineering of Open Fund of the Key Laboratory from Guangdong Province 2015.

References

- Dingle T, Wee S, Mulvey GL, Greco A, Kitova EN, Sun JX, Lin SJ, *et al.* Functional properties of the carboxyl-terminal host cell-binding domains of the two toxins, TcdA and TcdB, expressed by *Clostridium difficile*. *Glycobiology* 2008, 18: 698–706.
- Freeman J, Bauer MP, Baines SD, Corver J, Fawley WN, Goorhuis B, Kuijper EJ, *et al.* The changing epidemiology of *Clostridium difficile* infections. *Clin Microbiol Rev* 2010, 23: 529–549.
- Bauer MP, van Dissel JT, Kuijper EJ. *Clostridium difficile*: controversies and approaches to management. *Curr Opin Infect Dis* 2009, 22: 517–524.
- McFarland LV. Alternative treatments for *Clostridium difficile* disease: what really works? *J Med Microbiol* 2005, 54: 101–111.
- Alcantara C, Stenson WF, Steiner TS, Guerrant RL. Role of inducible cyclooxygenase and prostaglandins in *Clostridium difficile* toxin A induced secretion and inflammation in an animal model. *J Infect Dis* 2001, 184: 648–652.
- Yamada S, Maruyama I. HMGB1, a novel inflammatory cytokine. *Clin Chim Acta* 2007, 375: 36–42.
- Andersson U, Erlandsson-Harris H. HMGB1 is a potent trigger of arthritis. *J Intern Med* 2004, 255: 344–350.
- Wang H, Yang H, Tracey KJ. Extracellular role of HMGB1 in inflammation and sepsis. *J Intern Med* 2004, 255: 320–331.
- Porto A, Palumbo R, Pieron M, Aprigliano G, Chiesa R, Sanvito F, Maseri A, *et al.* Smooth muscle cells in human atherosclerotic plaques secrete and proliferate in response to high mobility protein box 1. *FASEB J* 2006, 20: E1–E9.
- Vakkila J, Lotze MT. Inflammation and necrosis promote tumor growth. *Nat Rev Immunol* 2004, 4: 641–648.
- Tsung A, Sahai R, Tanaka H, Nakao A, Fink MP, Lotze MT, Yang H, *et al.* The nuclear factor HMGB1 mediates hepatic injury after murine liver ischemia-reperfusion. *Archives* 2005, 201: 1135.
- Andrassy M, Volz HC, Igwe JC, Funke B, Eichberger SN, Kaya Z, Buss S, *et al.* High-mobility group box-1 in ischemia-reperfusion injury of the heart. *Circulation* 2008, 117: 3216–3226.
- Yu M, Wang H, Ding A, Golenbock DT, Latz E, Czura CJ, Fenton MJ, *et al.* HMGB1 signals through toll-like receptor (TLR4) and TLR2. *Shock* 2006, 26: 174–179.
- Girard JP. A direct inhibitor of HMGB1 cytokine. *Cell* 2007, 14: 345–347.
- Mollica L, Marchis FD, Spitaleri A, Dallacosta C, Pennacchini D, Zamai M, Agresti A, *et al.* Glycyrrhizin binds to high-mobility group box 1 protein and inhibits its cytokine activities. *Cell* 2007, 14: 431–441.
- Ii M, Matsunaga N, Hazeki K, Nakamura K, Takashima K, Seya T, Hazeki O, *et al.* A novel cyclohexene derivative, ethyl (6R)-6-[N-(2-Chloro-4-fluorophenyl) sulfamoyl]cyclohex-1-ene-1-carboxylate (TAK-242), selectively inhibits toll-like receptor 4-mediated cytokine production through suppression of intracellular signaling. *Mol Pharmacol* 2006, 69: 1288–1295.
- Vivot K, Langlois A, Bietiger W, Dal S, Seyfritz E, Pinget M, Jeandidier N, *et al.* Pro-inflammatory and pro-oxidant status of pancreatic islet *in vitro* is controlled by TLR-4 and HO-1 pathways. *PLoS One* 2014, 9: e107656.
- Chen RJ, Yuan HH, Zhang TY, Wang ZZ, Hu AK, Wu LL, Yang ZP, *et al.* Heme oxygenase-2 suppress TNF- α and IL6 expression via TLR4/MyD88-dependent signaling pathway in mouse cerebral vascular endothelial cells. *Mol Neurobiol* 2014, 50: 971–978.
- Sullivan NM, Pellett S, Wilkins TD. Purification and characterization of toxins A and B of *Clostridium difficile*. *Infect Immun* 1982, 35: 1032–1040.
- Kaur S, Vaishnavi C, Ray P, Kochhar R, Prasad KK. Effect of biotherapeutics on cyclosporin-induced *Clostridium difficile* infection in mice. *J Gastroenterol Hepatol* 2010, 25: 832–838.
- Stros M. HMGB proteins: interactions with DNA and chromatin. *Biochim Biophys Acta* 2010, 1799: 101–113.
- Chumbler NM, Farrow MA, Lapierre LA, Franklin JL, Haslam D, Goldenring JR, Lacy DB. *Clostridium difficile* toxin B causes epithelial

- cell necrosis through an autoprocessing-independent mechanism. *PLoS Pathog* 2012, 8: e1003072.
23. Bustin M. Regulation of DNA-dependent activities by the functional motifs of the high-mobility-group chromosomal proteins. *Mol Cell Biol* 1999, 19: 5237–5246.
 24. Sappington PL, Yang R, Yang H, Tracy KJ, Delude RL, Fink MP. HMGB1 B box increases the permeability of Caco-2 enterocytic monolayers and impairs intestinal barrier function in mice. *Gastroenterology* 2002, 123: 790–802.
 25. Deng Y, Yang Z, Gao Y, Xu H, Zheng B, Jiang M, Xu J, *et al.* Toll-like receptor 4 mediates acute lung injury induced by high mobility group box-1. *PLoS One* 2013, 8: e64375.
 26. Siemann M, Koch-Dorfler M, Rabenhorst G. *Clostridium difficile* associated diseases. The clinical courses of 18 fatal cases. *Intensive Care Med* 2000, 26: 416–421.
 27. Ryan A, Lynch M, Smith SM, Amu S, Nel HJ, McCoy CE, Dowling JK, *et al.* A role for TLR4 in *Clostridium difficile* infection and the recognition of surface layer proteins. *PLoS Pathogens* 2011, 7: e1002076.